Eur. Phys. J. D **20**, 297–304 (2002)
DOI: 10.1140/epjd/e2002-00135-x

THE EUROPEAN PHYSICAL JOURNAL D

Influence of the helium autoionization structures on the single/double ionization signal

L.A.A. Nikolopoulos[1,a], Takashi Nakajima[2], and P. Lambropoulos[1,3]

[1] Institute of Electronic Structure and Laser, FORTH, P.O. Box 1527, Heraklion, Crete 71110, Greece
[2] Institute of Advanced Energy, Kyoto University, Gokasho, Uji, Kyoto 611-0011, Japan
[3] Dept. of Physics, Univ. of Crete, P.O. Box 1527, Heraklion, Crete 71110, Greece

Received 19 February 2002 / Received in final form 2 May 2002
Published online 19 July 2002 –

Abstract. Calculations of intense field (around 10^{16} W/cm^2) single- and double-ionization processes in helium at XUV wavelengths are presented. The laser wavelength is chosen near the $|2s2p\ ^1\mathrm{P}\rangle$ autoionization structure and the dynamics are explored. Single and double ionization yields, as well as the photoelectron energy spectrum for photon energies around the autoionization structure are calculated. In the case of a pulse of few femtoseconds duration, no significant enhancement of the double ionization yield has been found in tuning the photon frequency around the peak of the resonance. It is also shown that in the case of a long pulse (and hence narrow compared with the relevant autoionization width), the branching ratio of double to single ionization yield can be relatively enhanced by tuning to the absorption minimum of the resonance.

PACS. 32.80.Rm Multiphoton ionization and excitation to highly excited states (e.g., Rydberg states) – 32.80.Dz Autoionization

1 Introduction

The interaction of short wavelength intense radiation with two-electron systems offers the possibility of exploring the interplay between correlation and double ionization in much more detail and depth than the study of single-photon double ionization can provide. This can be achieved through the study of few-photon double ionization in which, as has been discussed in recent work [1], correlation enters in many subtle ways, which are absent from single photon processes. Moreover, the judicious choice of the wavelength, even in a two-photon process, can affect the relative magnitude of the direct *versus* the sequential double electron ejection, an example of which has been discussed relatively recently [2].

A related question, that has been for quite some time lurking in the literature, is whether direct double ionization in a two-photon (or possibly few-photon) process can be enhanced by tuning the photon energy to an intermediate autoionizing resonance. This question has been explored most recently by Parker *et al.* [3] through their well established parallel computational approach [4,5] to the direct integration of the two-electron time-dependent Schrödinger equation. Specifically, they explored single and double ionization in helium under two-photon ionization for photon energies around single-photon resonance with the $|2s2p(^1\mathrm{P})\rangle$ doubly excited autoionizing state (AIS). Their final conclusion, reached through an application of their method to an *ab initio* as well as an one-electron model calculation of the helium, was that, whatever enhancement of double ionization was found, it was due to an increase of the sequential double ionization as the photon energy crosses the value of 54.4 eV, above which sequential double ionization becomes an overall two-photon process, whereas it is an overall three-photon process below that value. That is because for photon energies between ∼40 eV and ∼54.4 eV, it takes two photons to ionize He^+ from its ground state, a range of photon frequencies within which direct double ionization is relatively more pronounced, as discussed in detail by Kornberg and Lambropoulos [2].

Our purpose in this paper is to explore the vicinity of two autoionizing resonances in somewhat further detail, complementing thus the work of Parker *et al.* [3]. We have explored the same range of intensities, *i.e.* around 10^{16} W/cm^2. Noting, however, that even such high intensity in watts/cm^2 lies within the range of perturbative behaviour, owing to the large energy of the photons, we have performed our calculations through both the solution of the time dependent Schrödinger equation (TDSE) (in a limited but sufficient basis), as well as through a simplified few state model, whose chief use was to explore

[a] e-mail: nlambros@iesl.forth.gr

a further question; namely whether tuning the photon at the minimum of the autoionizing resonance, enhances in some way direct double ionization. Related to this question, one of us (TN) has recently studied the possibility of tuning a first laser to the absorption minimum of a low-lying autoionizing state, which is further coupled to a high-lying autoionizing state by a second laser, for the efficient pumping of high-lying autoionizing states [6]. Recall that, ideally, single-electron ionization (autoionization) at the minimum should be zero, leaving double ionization, for which the amplitude through the continuum (at the minimum) serves as a virtual intermediate state, unaffected. We do indeed find such a tendency, except that for a realistic excitation through a pulse, single-electron ejection for a frequency tuned at the minimum is not really zero, since the finite bandwidth of the pulse spans a range of frequencies around the minimum. Pursuing further the analysis of the excitation *via* a pulse, we have also studied the behaviour of the atom, through the photoelectron energy spectrum, for pulses such that their Fourier bandwidth may overlap more than one autoionizing resonance. The analysis of the photoelectron energy spectrum also complements that of Parker *et al.* [3], given that they present equivalent information at a larger photon frequency.

2 Formulation

We consider the helium in its ground state $(1s)^2\,{}^1\mathrm{S}_0$ in the presence of a field of frequency ω and N photons in the initial state. The states involved are the following :

$$\begin{aligned}
|g\rangle &= |\mathrm{He}(1s^2); N\rangle \equiv |(1s^2)\ {}^1\mathrm{S}; N\rangle \\
|a_1\rangle &= |\mathrm{He}(2s2p); N-1\rangle \equiv |2s2p\ {}^1\mathrm{P}; N-1\rangle \\
|a_2\rangle &= |\mathrm{He}(2s3p); N-1\rangle \equiv |2s3p\ {}^1\mathrm{P}; N-1\rangle \\
|c_1\rangle &= |\mathrm{He}^+(1s) + e^-_{\epsilon_1}; N-1\rangle \equiv |1s\epsilon_1 p\ {}^1\mathrm{P}; N-1\rangle \\
|c_2\rangle &= |\mathrm{He}^{++} + e^-_{\epsilon'_2} + e^-_{\epsilon_2}; N-2\rangle \equiv |\epsilon'_2 l' \epsilon_2 l,\ {}^1\mathrm{S}({}^1\mathrm{D}); N-2\rangle \\
|c_3\rangle &= |\mathrm{He}^+(1s) + e^-_{\epsilon_3}; N-2\rangle \equiv |1s\epsilon_3 s, (d)^1\mathrm{S}({}^1\mathrm{D}); N-2\rangle \cdot
\end{aligned} \tag{1}$$

Representation of the states (atom + field) in this way implies the quantized form of the electromagnetic field (E/M), which although not necessary, is convenient for our formulation. The photon energy of the field is sufficient to ionize helium from its ground state raising one of the electrons in the (^{1}P) continuum with kinetic energy ϵ_1 and simultaneously exciting the system to the autoionization resonances $\mathrm{He}(2s2p), \mathrm{He}(2s3p)$ from which it can decay into the continuum $|c_1\rangle$, due to the electron-electron interaction operator $V = 1/|\mathbf{r}_1 - \mathbf{r}_2|$. Furthermore the system can absorb one more photon, reaching thus the double ejection threshold, either through absorption from the He^+ ground state (sequential path) or from the autoionizing states $|a_1\rangle$ and $|a_2\rangle$. The kinetic energies of the photoelectrons in those cases are denoted by $\epsilon_i, i = 1, 2, 3$. With l, l' we denote the quantum angular momentum number of the photoelectrons.

The Hamiltonian of the system is $H = H_A + H_R + D + V = H_0 + D + V$ where H_A and H_R are the field-free atomic Hamiltonian and the free E/M field respectively. The operator D is the interaction between the atom and the external laser field in the dipole approximation. The non-zero couplings between the discrete states $|g\rangle, |a_1\rangle, |a_2\rangle$ and the continuum states $|c_i\rangle, i = 1, 2, 3$ are the following:

$$\begin{aligned}
&\langle g|H|c_1\rangle = D_{gc_1}, \quad \langle a_i|H|c_j\rangle = D_{ic_j}, \quad i = 1, 2 \quad j = 2, 3 \\
&\langle a_i|H|c_1\rangle = V_{ic_1}, \quad i = 1, 2, \quad \langle c_1|H|c_j\rangle = D_{1c_j}, \quad j = 2, 3.
\end{aligned}$$

Note here that the discrete doubly excited states we assume are those obtained when the interelectronic interaction $V_{a_1 a_2}$ has been taken into account only between the discrete states. In other words, we assume that the discrete and the continuum states, involved in the model, satisfy the following orthonormality relations:

$$\begin{aligned}
&\langle g|H|g\rangle = E_g, \qquad \langle a_i|H|a_j\rangle = E_{a_i}\delta_{ij}, \qquad i, j = 1, 2 \\
&\langle E'_{c_i}|H|E_{c_i}\rangle = E_{c_i}\delta(E'_{c_i} - E_{c_i}), \qquad i = 1, 2, 3.
\end{aligned}$$

In the above subspace, the most general form of the state of the system in time t will be of the form:

$$\begin{aligned}
|\psi(t)\rangle = U_g(t)|g\rangle &+ \sum_{i=1,2} U_{a_i}(t)|a_i\rangle \\
&+ \sum_{i=1,2,3} \int \mathrm{d}E_{c_i} U_{c_i}(E_{c_i}, t)|c_i\rangle \cdot
\end{aligned} \tag{2}$$

Our task is to determine the time evolution of the state $\psi(t)$ through the amplitudes $U_\mu(t)$ ($\mu \equiv g, a_i, c_j$, $i = 1, 2$, $j = 1, 2, 3$), which allow us to calculate the population of the ground state and the population in each of the continua involved, as a function of the photoelectron energy (PES). The dynamics of the system is governed by the TDSE which reads:

$$\mathrm{i}\frac{\partial}{\partial t}|\psi(t)\rangle = [H_0 + D(t) + V]\,|\psi(t)\rangle, \quad |\psi(t=0)\rangle \equiv |g\rangle \cdot \tag{3}$$

Inserting equation (2) into equation (3) we obtain a system of first order integro-differential equations for the amplitudes of the state vector $U_\mu(t)$ ($\mu \equiv g, a_1, a_2, c_1, c_2, c_3$). The various couplings between states involving continua complicate the problem considerably, since the time evolution of each amplitude depends on the time evolution of an infinite number of states (the continuum states).

To first approximation, when the couplings D are assumed to be of constant magnitude, as in the case of a square pulse, the resulting TDSE can be solved analytically. In the general case, however, the classical limit of a quantized field linearly polarized, is of the form $E(t) = E_0(t)\cos\omega t$, We shall assume for the moment a pulse with constant amplitude, namely $E_0(t) = E_0$. This way we can transform the equations using the Laplace operator and once the continua have been eliminated (with their contribution reduced to an ionization width of the discrete states of the system), by making the inverse Laplace-transform

we obtain a simplified system of first-order ordinary differential equations [7].

For a constant perturbation, the TDSE (Eq. (3)), after performing the Laplace-transform, is transformed to an algebraic equation for the resolvent operator $G(z)$, $(z - H_0 - D - V)G(z) = \mathbf{1}$, with z being a complex number. If the time evolution operator of the system is denoted by $\hat{U}(t)$, then the time-dependent wavefunction is determined by $\psi(t) = \hat{U}(t)\, t\psi(0) = \hat{U}(t)|g\rangle$. The matrix elements of the evolution operator for the various states of the system (given the initial conditions) are obtained as the inverse Laplace transform of $G(z)$, namely:

$$U_\mu(t) = -\frac{1}{2\pi \mathrm{i}} \lim_{\eta\to 0^+} \int_{-\infty}^{+\infty} \mathrm{d}y\; G_\mu(y + \mathrm{i}\eta)\mathrm{e}^{-\mathrm{i}yt}. \quad (4)$$

For notational brevity we write the matrix elements of $G(z)$ as, $G_\mu \equiv G_\mu(z) = \langle\mu|G(z)|g\rangle$. Writing $(z - H_0 - D)\,\mathbf{1}\,G(z)|g\rangle = |g\rangle$ and projecting the states $\langle g|$, $\langle a_1|$, $\langle a_2|$, $\langle c_1|$, $\langle c_2|$, $\langle c_3|$ we obtain for the amplitudes G_g, G_{a_1}, G_{a_2}, G_{c_1}, G_{c_2}, G_{c_3}, a system of algebraic equations, from which, following the standard procedure [9], we substitute the amplitudes G_{c_i}, $i = 1, 2, 3$ of the continuum states into the equations for the discrete states amplitudes G_g, G_{a_1}, G_{a_2}, we obtain:

$$\left[z - E_g - \int \mathrm{d}E_{c_1} \frac{|D_{gc_1}|^2}{z - E_{c_1}}\right] G_g \sum_{i=1,2} \left[D_{ga_i} + \int \mathrm{d}E_{c_1} \frac{D_{gc_1}V_{c_1a_i}}{z - E_{c_1}}\right] G_{a_i} = \mathbf{1} \quad (5)$$

$$-\left[D_{a_1g} + \int \mathrm{d}E_{c_1} \frac{V_{a_1c_1}D_{c_1g}}{z - E_{c_1}}\right] G_g + \left[z - E_{a_1} - \int \mathrm{d}E_{c_1} \frac{|V_{c_1a_1}|^2}{z - E_{c_1}}\right] G_{a_1} - \Omega_{12}G_{c_2} = 0 \quad (6)$$

$$-\left[D_{a_2g} + \int \mathrm{d}E_{c_2} \frac{V_{a_2c_1}D_{c_1g}}{z - E_{c_1}}\right] G_g + \left[z - E_{a_2} - \int \mathrm{d}E_{c_1} \frac{|V_{c_1a_2}|^2}{z - E_{c_1}}\right] G_{a_1} - \Omega_{21}G_{c_1} = 0 \quad (7)$$

$$-D_{c_1g}G_g + \left[z - E_{c_1} - \int \frac{|D_{c_2c_1}|^2}{z - E_{c_2}}\right] G_{c_1} - \sum_{i=1,2} V_{c_1a_i}G_{a_i} = 0 \quad (8)$$

$$-\sum_{i=1,2} D_{c_2a_i}G_{a_i} - \int \mathrm{d}E_{c_1} D_{c_2c_1}G_{c_1} + (z - E_{c_2})G_{c_2} = 0 \quad (9)$$

$$-\sum_{i=1,2} D_{c_3a_i}G_{a_i} + (z - E_{c_3})G_{c_3} = 0. \quad (10)$$

By making the pole approximation $z \to E_g + \omega + \mathrm{i}\eta$ at the limit of $\eta \to 0$, we see that the integrals obtain a real and imaginary part. The next step in the calculation, following Fano's original paper [8] (Sect. 5), is to take into account the effect of the second-order interaction Ω_{12}, namely,

$$\Omega_{12} = \int \mathrm{d}E_{c_1} \frac{V_{a_1c_1}V_{c_1a_2}}{z - E_{c_1}} G_{c_2} = P\int \mathrm{d}E_{c_1} \frac{V_{a_1c_1}V_{c_1a_2}}{z - E_{c_1}} G_{c_2} - \mathrm{i}\pi V_{a_1c_1}V_{c_1a_2}|_{E=E_g+\omega} \quad (11)$$

upon the discrete states $|a_1\rangle, |a_2\rangle$. Note that the quantity Ω_{21} is obtained by interchanging the states $|a_1\rangle, |a_2\rangle$ in Ω_{12}. Thus, we diagonalize the sub-Hamiltonian, acting on those states and we obtain a new set of discrete states $|\bar{a}_1\rangle, |\bar{a}_2\rangle$ with new eigenenergy positions $E_{\bar{a}_1}, E_{\bar{a}_2}$. The real part of this quantity is absorbed into the new eigenenergies; which should be the position of the physically observable resonances in photoabsorption. Next, we transform the resulting equations back into the time-domain by making the inverse Laplace-transform thus obtaining the following system of first-order ordinary differential equations for the amplitudes:

$$\begin{aligned}
\mathrm{i}\frac{\mathrm{d}}{\mathrm{d}t}U_g(t) &= \left[E_g + S_g(t) - \mathrm{i}\frac{\gamma_g(t)}{2}\right] U_g(t) + \sum_{i=1,2} \bar{\Omega}_i(t)U_{\bar{a}_i}(t)\\
\mathrm{i}\frac{\mathrm{d}}{\mathrm{d}t}U_{\bar{a}_1}(t) &= \left[E_{\bar{a}_1} - \mathrm{i}\frac{\Gamma_{\bar{a}_1}(t)}{2}\right] U_{\bar{a}_1}(t) + \bar{\Omega}_1(t)U_g(t) + \mathrm{i}\Omega_{12}^I U_{\bar{a}_2}\\
\mathrm{i}\frac{\mathrm{d}}{\mathrm{d}t}U_{\bar{a}_2}(t) &= \left[E_{\bar{a}_2} - \mathrm{i}\frac{\Gamma_{\bar{a}_2}(t)}{2}\right] U_{\bar{a}_2}(t) + \bar{\Omega}_2(t)U_g(t) - \mathrm{i}\Omega_{12}^I U_{\bar{a}_1}\\
\mathrm{i}\frac{\mathrm{d}}{\mathrm{d}t}U_{c_1}(t) &= \left[E_{c_1} - \mathrm{i}\frac{\gamma_1(t)}{2}\right] U_{c_1}(t) + \sum_{i=1,2} V_{c_1\bar{a}_i}U_{\bar{a}_i}(t) + D_{c_1g}(t)U_g(t)\\
\mathrm{i}\frac{\mathrm{d}}{\mathrm{d}t}U_{c_j}(t) &= E_{c_j}U_{c_j}(t) + \sum_{i=1,2} D_{c_j\bar{a}_i}(t)U_{\bar{a}_i}(t) \quad (j = 2, 3).
\end{aligned}$$

In the expansion (2) the states $|a_i\rangle, i = 1, 2$ are replaced by the new states $|\bar{a}_i\rangle, i = 1, 2$ and accordingly in the differential equations above appear the new coefficients $U_{\bar{a}_1}, U_{\bar{a}_2}$. The imaginary part of the integrals over the continuum states have been reduced to time-dependent coarse graining widths (denoted by γ_1, γ_g and $\Gamma_{\bar{a}_1}, \Gamma_{\bar{a}_2}$), while the real part to energy shifts as follows:

$$S_g(t) = \fint \mathrm{d}E_{c_1} \frac{|D_{gc_1}|^2}{E_g + \omega - E_{c_1}}, \quad (12)$$

$$\gamma_g(t) = 2\pi\left|D_{gc_1}(E_{c_1} = E_g + \omega)\right|^2, \quad (13)$$

$$\gamma_1(t) = 2\pi|D_{c_1c_2}(E_{c_2} = E(\mathrm{He}^+(1s)) + \omega)|^2 \quad (14)$$

and

$$\Gamma_{\bar{a}_i}(t) = \Gamma_1 + \sum_{j=2,3} \gamma_{\bar{a}_{ij}}(t) \tag{15}$$

$$\gamma_{\bar{a}_{ij}}(t) = 2\pi |D_{\bar{a}_i c_j}(E_{c_j} = E_{\bar{a}_i} + \omega)|^2, \quad (j = 2, 3) \tag{16}$$

$$\Gamma_1 = 2\pi |V(E_{c_1} = E_g + \omega)|^2, \tag{17}$$

with $i = 1, 2$. Finally the quantities $\bar{\Omega}_i,\ i = 1, 2$ are the complex Rabi frequencies, characteristic of autoionization, defined by:

$$\begin{aligned} \bar{\Omega}_i &= \Omega_i(t) \left(1 - \frac{\mathrm{i}}{q_i}\right) \\ &\equiv D_{g\bar{a}_i}(t) + \lim_{\eta \to 0^+} \sum\!\!\!\!\!\!\int \frac{D_{gc_1}(t) V_{c_1 \bar{a}_i}}{E_g + \omega - E_{c_1} + \mathrm{i}\eta}, \\ &\quad i = 1, 2 \end{aligned} \tag{18}$$

where $\Omega_{12}^I = -\sqrt{\Gamma_1 \Gamma_2}/2$ is the imaginary part of the complex quantity defined by (11). while the quantities $q_i, i = 1, 2$ are the Fano q-parameters [8] defined by inspection of relation (18). We should keep in mind here that the Fano q-parameters are time-independent quantities. Note that the amplitudes have to satisfy the normalization condition,

$$|U_g(t)|^2 + \sum_{i=1,2} |U_{\bar{a}_i}(t)|^2 + \sum_{i=1,2,3} \int \mathrm{d}E_{c_i} |U_{c_i}(E_{c_i}, t)|^2 = 1. \tag{19}$$

A brief digression into formalism may be useful at this point in order to underscore the validity of the formulation employed in this work. The separation of the wavefunction into discrete and continuum parts entails a partition of the atomic Hamiltonian, which in one form or another is involved in any method. If the partition of the Hamiltonian is chosen judiciously the energy positions of the states $|\bar{a}_1\rangle$ and $|\bar{a}_2\rangle$ should coincide with the positions of the observed resonances *i.e.* the physical states. In a somewhat different formulation, which stresses this physical picture, one can consider the physical states Ψ_E in the continuum which, however, is not smooth due to the presence of the resonances. Then the matrix element $\langle \Psi_E | D | g \rangle$ will not be a smooth function of the energy E, as it will exhibit resonances. In the vicinity of two resonances, relatively isolated form others, it can be written as,

$$\langle \Psi_E | D | g \rangle = -D_{cg} \frac{1 + \dfrac{q_1}{\epsilon_1} + \dfrac{q_2}{\epsilon_2}}{\left[1 + \left(\dfrac{1}{\epsilon_1} + \dfrac{1}{\epsilon_2}\right)^2\right]^{1/2}}, \tag{20}$$

with q_1, q_2 being the q-parameters of the resonances and ϵ_1, ϵ_2 the dimensionless detuning of the radiation from the respective resonances measured in units of the respective widths, and D_{cg} the direct dipole matrix element into the smooth uncoupled continuum. This expression, which is valid when two resonances decay into one and the same continuum can be easily generalized to more resonances. One can, after a considerable amount of algebra (which we refrain from reproducing here) show that the formulation in equation (10) is equivalent, in the sense that it leads to the above expression. This implies that in the formulation of Section 2, we can interpret the energy positions of $|\bar{a}_1\rangle$ and $|\bar{a}_2\rangle$ as those of the physical resonances, which we obtain through a separate atomic calculation together with the corresponding q-parameters and autoionization widths. The main point of this digression is to show that the imaginary parts of the cross terms Ω_{12} are present because of the particular formulation, while the real parts must be absorbed into the energy positions of the physical resonances, in any formalism. The complete equivalence of these two formalisms, in the case of single resonances, have been discussed in detail long ago [9].

Now we are in the position to consider a pulse with time-dependent profile better suited, than the square pulse, for more realistic situations. After the end of the pulse, the time-dependent coefficients provide the populations of the respective states of the system. The population of He^{++}, He^+ and of the ground state of He, for long times, are related by $P_g + P(He^+) + P(He^{++}) = 1$. The photoelectron energy spectrum (PES) is defined as the population of the continuum in the long-time limit (in practice at the end of the pulse), given by:

$$S(\epsilon_c) = \lim_{t \to \infty} \left[\sum_{i=1,2,3} |U_{c_i}(E_{c_i}, t)|^2 \right]. \tag{21}$$

From here on, for notational brevity, we shall denote the new eigenstates by $|a_1\rangle, |a_2\rangle$ instead of $|\bar{a}_1\rangle, |\bar{a}_2\rangle$.

2.1 Simplified system

To the extent that the inclusion of a single autoionizing state is sufficient to gain some insight into the dynamics of the system, the set of equations given in the previous subsection can be simplified so that we can obtain analytical expressions under certain conditions. Assuming that the laser frequency is near resonant with the $|2s2p\ ^1\mathrm{P}_1\rangle$ state, we neglect $|a_2\rangle$ in the analysis that follows in this subsection ($|\bar{a}_1\rangle \equiv |a_1\rangle$). Note also, that the continuum-continuum transition ($|c_1\rangle \to |c_2\rangle$) has been neglected. As a result, the single- and the double-ionization do not interfere with anything. Introducing the slowly-varying amplitudes $u_g = U_g \mathrm{e}^{\mathrm{i}E_g t}, u_{a_1} = U_{a_1} \mathrm{e}^{\mathrm{i}(E_g + \omega)t}$ for the two discrete states, the simplified equations are written as,

$$\dot{u}_g = -\frac{1}{2}\gamma_g u_g - \mathrm{i}\Omega_1 \left(1 - \frac{\mathrm{i}}{q_1}\right) u_a \tag{22}$$

$$\dot{u}_{a_1} = \left[\mathrm{i}\delta - \frac{1}{2}\Gamma_{a_1}\right] u_{a_1} - \mathrm{i}\Omega_1 \left(1 - \frac{\mathrm{i}}{q_1}\right) u_g \tag{23}$$

$$\dot{U}_{c_1} = \mathrm{i}E_{c_1} U_{c_1} - \mathrm{i}D_{c_1 g} U_g - \mathrm{i}V_{c_1 a_1} U_{a_1} \tag{24}$$

$$\dot{U}_{c_j} = -\mathrm{i}E_{c_j} U_{c_j} - \mathrm{i}D_{c_j a_1} U_{a_1}, \qquad (j = 2, 3) \tag{25}$$

with $\delta = E_g + \omega - E_{a_1}$. Note that all quantities appearing in the above equations have been defined in the previous subsection.

Before proceeding further, a comment on the treatment of the double continuum c_3 is necessary. Strictly speaking, it is not correct to treat $|c_3\rangle$ as if it were a single continuum, since it involves two continua. In the present case, however, this is legitimate since we do not consider the photoelectron energy spectrum above the double ionization threshold. We are here interested only in the total double ionization yield. In other words, after integrating $|U_{c_2}|^2$ over photoelectron energy E_{c_2}, we obtain the correct population into $\{|c_2\rangle\}$. We also assume that all ions associated with the $|c_1\rangle$ continuum have a core He($1s$), *i.e.*, we ignore the branching into the He($2s$) ionic core, which in the present context can be shown to be negligible.

We define now R_1 and R_2 as single- and double-ionization yields. It should be kept in mind that R_1 contains all contributions to photoionization; from $|g\rangle$ (into $|c_1\rangle$), autoionization from $|a_1\rangle$ (into $|c_1\rangle$), and single-photon ionization from $|a_1\rangle$ (into $|c_3\rangle$), while R_2 represents, a sequential double-ejection process with photoionization width $\gamma_{a_1}^{++}$. Then, we obtain,

$$\dot{R}_1 = \frac{\mathrm{d}}{\mathrm{d}t}\int \mathrm{d}E_{c_1}|U_{c_1}|^2 + \frac{\mathrm{d}}{\mathrm{d}t}\int \mathrm{d}E_{c_3}|U_{c_3}|^2 - \gamma_1 R_1 \quad (26)$$

$$\dot{R}_2 = \frac{\mathrm{d}}{\mathrm{d}t}\int \mathrm{d}E_{c_2}|U_{c_2}|^2 + \gamma_1 R_1. \quad (27)$$

In the above equation for R_2, the first term represents the direct, while the second term represents the sequential process.

In general, using Laplace transform, equations (25) can be solved analytically for a square pulse. Using the solution thus obtained for u_g and u_{a_1}, expressions for U_{c_j} ($j = 1, 2, 3$) can be obtained. Next, a coarse grained rate can be derived from the expression,

$$\dot{R}_1 = \frac{1}{\delta t}\int \mathrm{d}E_{c_1}\left(|U_{c_1}(t+\delta t)|^2 - |U_{c_1}(t)|^2\right) + \frac{1}{\delta t}\int \mathrm{d}E_{c_3}\left(|U_{c_3}(t+\delta t)|^2 - |U_{c_3}(t)|^2\right) - \gamma_1 R_1 \quad (28)$$

$$\dot{R}_2 = \frac{1}{\delta t}\int \mathrm{d}E_{c_2}\left(|U_{c_2}(t+\delta t)|^2 - |U_{c_2}(t)|^2\right) + \gamma_1 R_1. \quad (29)$$

It should be evident that, each expression for U_{c_j} ($j = 1, 2, 3$) will consist of three exponential terms with $\mathrm{e}^{-s_+ t}$, $\mathrm{e}^{-s_- t}$, and $\mathrm{e}^{-\mathrm{i}\delta_{c_j} t}$ where $s_\pm$ are the roots of

$$\left(s + \frac{1}{2}\gamma_g\right)\left[s - \mathrm{i}\delta + \Gamma_{a_1})\right] \equiv (s - s_+)(s - s_-) = 0. \quad (30)$$

If the field is sufficiently weak, in the sense that Rabi oscillations between $|g\rangle$ and $|a_1\rangle$ are not significant, and the interaction time τ is such that $\Gamma_1\tau \gg 1$ but $\gamma_g\tau \ll 1$, only the terms involving $\mathrm{e}^{-s_- t}$ survive in equations (28, 29). Then, we obtain,

$$\dot{R}_1 = 2\pi\left[\left|\frac{D_{c_1 g}\left\{-s_- + \mathrm{i}\delta - (\gamma_{a_1}^{+} + \gamma_{a_1}^{++})/2\right\} + \mathrm{i}V_{c_1 a_1}\Omega}{s_+ - s_-}\right|^2 + \left|\frac{D_{c_3 a_1}\bar{\Omega}_1}{s_+ - s_-}\right|^2\right]\mathrm{e}^{2Res_- t} - \gamma_1 R_1 \quad (31)$$

$$\dot{R}_2 = 2\pi\left|\frac{D_{c_2 a_1}\bar{\Omega}_1}{s_+ - s_-}\right|^2 \mathrm{e}^{2Res_- t} + \gamma_1 R_1\,. \quad (32)$$

Finally, the single- and double-ionization rates $\dot{R}_1$ and $\dot{R}_2$ can be obtained as,

$$\dot{R}_1|_{t=0} = \left|\frac{D_{c_1 g}\delta + V_{c_1 a_1}\Omega_1}{\delta + \mathrm{i}\Gamma_1/2}\right|^2 + \left|\frac{D_{c_3 a_1}\bar{\Omega}_1}{\delta + \mathrm{i}\Gamma_1/2}\right|^2 \quad (33)$$

$$\dot{R}_2|_{t=0} = \left|\frac{D_{c_2 a_1}\bar{\Omega}_1}{\delta + \mathrm{i}\Gamma_1/2}\right|^2. \quad (34)$$

Obviously, these results suggest that, in the weak field limit which, should be emphasized again, is valid for rather large values of the intensity in W/cm^2 at this photon energy, the direct double ionization yield into the $|c_2\rangle$ continuum *via* $|a_1\rangle$ as a function of the laser detuning from the autoionizing resonance, has a Lorentzian profile with width Γ_1. The single ionization yield *via* $|a_1\rangle$ (*i.e.*, into the $|c_3\rangle$ continuum) has a profile identical to that of the direct double ionization. This branching depends on the ratio of the matrix elements $D_{c_3 a_1}$ and $D_{c_2 a_1}$ and is independent of δ.

On the other hand, the single photoionization into the $|c_1\rangle$ continuum has the usual autoionization line profile whose asymmetry is determined by q_1. This means that, although the main contribution to double ionization comes from the sequential process and also the direct double ionization itself is maximum at $\delta = 0$, the ratio between sequential and direct double ionization would be smallest at the absorption minimum; simply because single electron ejection is minimized at the minimum.

2.2 Atomic basis

In order to obtain the necessary atomic parameters for helium, we have calculated the field-free multichannel states ψ_E^i where i indicates a channel associated with a certain ionic eigenstate denoted by Φ_i [1] and E the energy of the atomic system. This ionic eigenstate can be either a bound or a continuum state of the ion. The method through which we obtain these multichannel states has been presented and employed for single-photon double ionization [10], as well as two-photon double ionization [1] of helium, within lowest order perturbation theory (LOPT). Briefly, the channels $\psi_E^i \equiv |ELSM_L M_S; \Phi_i, \epsilon' l'\rangle$ contributing to the final state are characterized by the quantum numbers of the core target state Φ_i, namely the energy and the angular momentum (ϵ, l), as well as the quantum numbers of the other electron (ϵ', l'), subject to

the relation $\epsilon+\epsilon' = E$, and with l and l' restricted by angular momentum and parity addition rules so as to result to a state with L, S angular and spin momenta. Since we construct the target (one-electron) states $\Phi_i(\epsilon, l\rangle)$ as solutions of the He^+ Hamiltonian, the resulting discrete eigenenergies ϵ are negative and positive. The negative ones correspond to the bound spectrum while the positive ones to the continuous spectrum. We separate single from double ejection final states as follows: final channel states with one-electron core states and ϵ negative ($\epsilon < 0$) contribute to single ejection, while all of the rest ($\epsilon > 0$) contribute to double ejection. With the above in mind, the algorithm for calculating the multichannel states ψ_E^i is the following: We first construct the bound states of the system using fixed boundary conditions [10], namely the two-electron wavefunctions are assumed confined in a spherical box of radius $R = 40$ a.u. with nodes at the two edges $\psi(0,0) = \psi(0,R) = \psi(R,R) = 0$. Next, the multichannel continuum states are calculated with no assumed boundary conditions for the symmetries $L = 0, 1, 2$. Having obtained the above two-electron, field-free LS-uncoupled states, we are in the position to calculate the corresponding dipole matrix elements between those states. Those dipole matrix elements and the energies of the two-electron states are the only dynamical quantities that enter the equations for the time-dependent coefficients. Since we confine the basis employed here to $L_{\max} = 2$, the importance of processes such as two-electron ATI, noted by Parker *et al.* [3], cannot be assessed quantitatively nor it is within our purposes here.

3 Results and discussion

First we assume, as in the work of Parker *et al.* [3] a laser pulse of trapezoidal profile, with peak intensity $I_0 = 4 \times 10^{16}$ W/cm^2 and of photon energy on resonance with the $|2s2p\rangle$ autoionizing state (AIS) of helium. The laser pulse is ramped on and off over 8 cycles, with a total duration of 25 cycles.

In Figure 1 we present the population of the discrete states of the system (ground + model autoionizing states). The figure is quite similar to that produced by Parker *et al.*, as obtained from the direct integration of the two-electron time-dependent Schrödinger equation. Basically, the results are identical, with a difference in the population decay after the end of the pulse. It is evident that after the passage of the pulse, the populations at the two AIS will decay with a half-life equal to $1/\Gamma_1$ for the first and $1/\Gamma_2$ for the second state. However, the population of the AIS $|a_2\rangle$, as obtained here is not large enough (compared to the population of the AIS $|a_1\rangle$) to produce the oscillations found in [3]. The oscillations we find are reduced by more than an order of magnitude, compared to those in Parker *et al.* [3], which may be due to the difference in the methods of calculation, as well as in the analysis of the final information.

Although, regarding the atomic structure, no compromises have been made (except computational limits), since the method we have developed produces two-electron correlated states in a fully *ab initio* way, the reduction of the Hamiltonian space involved in the dynamics makes our approach complementary to that work. Our approach, however, provides detailed information about some quantities of interest in single and double ionization of helium, near resonances. One such quantity is the PES, which was one of the objectives of this work, namely to examine the behaviour of the PES near an autoionizing resonance and its role in the single and double ionization signal, as a function of various parameters of the pulse. Related information for photon energy 3.2 a.u. has also been given in Parker *et al.* [3].

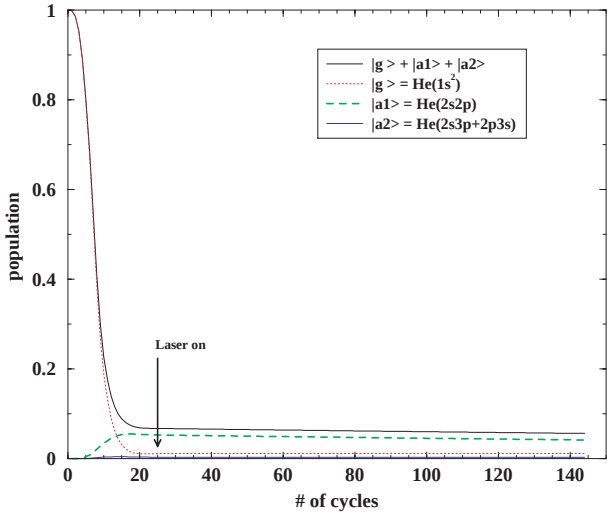

Fig. 1. Population of the discrete states of the system during the a laser pulse of wavelength 20.6 nm and of peak intensity 4×10^{16} W/cm^2. The pulse shape is trapezoidal and ramped on and off over 8 cycles, with a total duration of 25 cycles. The arrow in the figure denotes the time that the laser stops acting on the system. Interaction between the excited electrons is then responsible for the change of the populations at subsequent times.

In Figure 2, we show the photoelectron energy spectra at two different times. The full curve is the population into the continuum, at the end of pulse (after 25 cycles of the field) while the other is at a time that corresponds to 900 cycles. Since after 25 cycles the field is zero, whatever photoelectrons are produced between that time and 900 cycles come from autoionization. The shape of this PES is rather reasonable if one considers the strength of the autoionization compared with the pulse duration as well as with the peak intensity. Given that the width of the resonant AIS is $\Gamma_1 \sim 1.3 \times 10^{-3}$ in a.u. we find a life time of the order $\tau_1 \sim 17.61$ fs. The laser is on for 25 cycles ($\tau_{\rm L} \sim 1.72$ fs), which means spectral width of about $\Delta\omega \sim 1/\tau_{\rm L} = 2.4$ eV; the interaction time is about 10 times smaller than the AIS width, $\Gamma_1\tau_{\rm L} \sim 0.1$. Given the spectral width of the pulse, we see that it is broad enough to populate both AIS $|a_1\rangle, |a_2\rangle$ taking also into account the relative shift of the ground state $S_g \sim 0.13I_0 = 4.03$ eV and the ponderomotive shift of the states above the first ionization threshold, $U_p \sim I_0/4\omega^2 = 1.588$ eV. At the end of the pulse, the maximum population in the continuum is shifted because

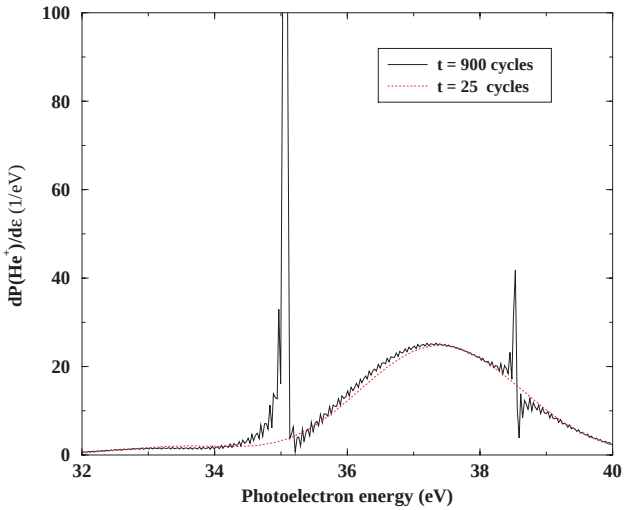

Fig. 2. Photoelectron energy spectra at two different points in time after the laser started acting on the system. The dotted line represents the energy distribution of the photoelectron for energy range around the position of the autoionizing structures at time equal to 25 cycles of the field. The full curve is the same quantity as evolved to time equal to 900 cycles of the field. Note that the autoionization lifetime of the state $|2s2p\rangle$ is about 250 cycles.

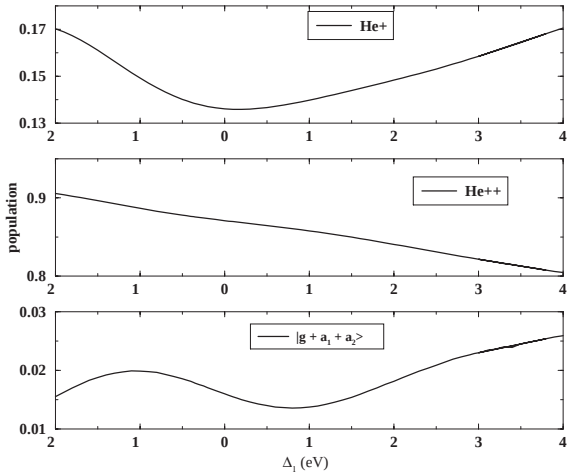

Fig. 3. Populations of the He^+, He^{++} and bound states of helium as a function of the laser detuning from the AIS $|2s2p\rangle$ at time of about 900 cycles of the field. For comparison the AIS width is about 250 cycles. The pulse duration was 25 cycles.

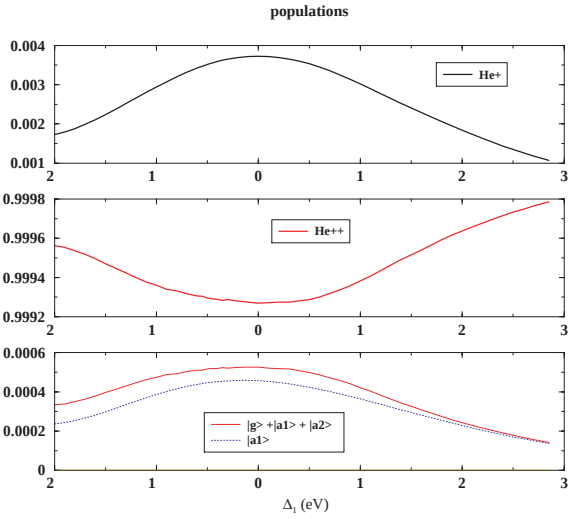

Fig. 4. Same as the previous figure, with pulse duration about 250 cycles.

of those shifts. After turning off the laser, the only channel of populating the continuum is the electron-electron interaction, peaked at the field-free AIS energy positions; and this is the case as shown in the figure. The oscillations in the dotted curve are due basically to the finite duration of the pulse and generally decay, provided we look at times long compared with the AIS width ($t \gg 1/\Gamma_1, 1/\Gamma_2$). Elementary analysis of the differential equations for such times gives for the PES:

$$S(E_{c_1}, t) \sim t^2 \left[\Gamma_1 |U_{a_1}|^2 \frac{\sin^2(\Delta_{a_1} t/2)}{(\Delta_{a_1} t/2)^2} + \Gamma_2 |U_{a_2}|^2 \frac{\sin^2(\Delta_{a_2} t/2)}{(\Delta_{a_2} t/2)^2} \right] \quad (35)$$

with $\Delta_{a_i} \equiv E_{c_1} - E_{a_i}$, $i = 1, 2$. From this equation, the origin of the oscillation becomes evident, as well as the peak structures in the limit of $\Delta_{a_i} t \to 0$.

In Figure 3, we show the populations of the He^+, He^{++} and discrete states as a function of the detuning with the AIS $|a_1\rangle$ at 900 cycles of the field period ∼62.15 fs; *i.e.* about three times the width of state $|a_1\rangle$. From the figure, we see that none of those curves exhibits the typical Fano profile [8]. This behaviour is not unexpected, given the small (compared to $1/\Gamma_1$) interaction time. On the other hand, the peak intensity of the pulse is 4.0×10^{16} W/cm^2 which makes the maximum Rabi strength $\Omega_1 \sim 0.0227\sqrt{I_0} = 0.0295$, about 17 times larger than Γ_1; namely $\Omega_1 = 17.15\Gamma_1$. It has been shown by Lambropoulos and Zoller (see discussion of Fig. 4 in [9]), that when the interaction time is much less than the autoionization lifetime even a moderately strong intensity can modify considerably the weak-field typical Fano line profile. For the present laser parameters the population for He^{++} is not affected by the presence of the AI states. We should note here, that the He^{++} population remains constant with the end of the pulse while the He^+ increases depending on the observation time. Eventually, within our model, in times of the order of a few AIS widths $1/\Gamma_1$ the population in He^+ will be that of population of He^+ plus the population of AIS at the end of the pulse. The main channel of production of He^{++} is the sequential channel and the decrease of He^{++} population as a function of the photon energy is due to the corresponding decrease in the rate γ_1.

In Figure 4 we present calculations similar to those of Figure 3 but with duration of the laser about 250 cycles (∼17.2 fs), almost equal to the width of AIS $|a_1\rangle$. The results change, when crossings the AIS $|a_1\rangle$, in contrast of those of the smaller duration pulse. The population of He^+

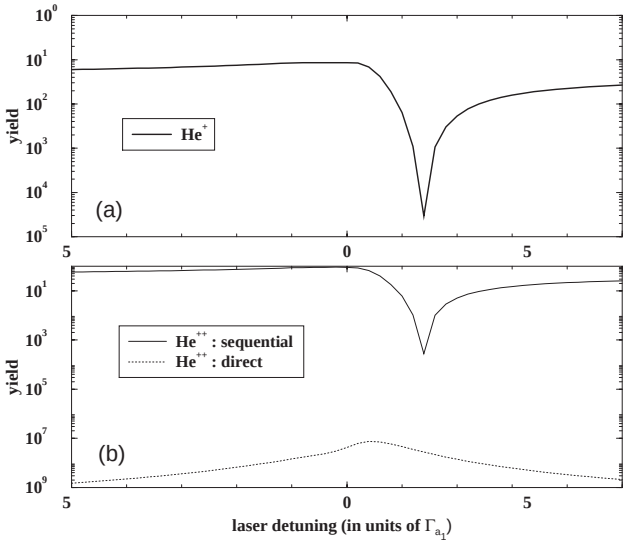

Fig. 5. Variation of the ionization yields as a function of laser detuning for a 1 ps Gaussian pulse at the intensity of 4×10^{11} W/cm^2. (a) Single ionization yield and (b) sequential- and direct-double ionization yields.

and of the discrete state have the same behaviour and a clear increase (though rather broad) occurs for near resonance photon energies. Most of the discrete states population is in the AIS state, which eventually will decay to the He^+ continuum. This channel affects the He^{++} population in the opposite way, since crossing the resonance a broad minimum appears. The PES, not presented here, exhibits two narrow peaks, in a rather smooth background, at the energy positions of the AIS $|a_1\rangle$ and $|a_2\rangle$, in accordance with the large duration of the laser pulse. Basically, in both cases, though with different response to the laser pulse, not significant enhancement of He^{++} can be attributed to the presence, of the resonances. For reasonable laser pulse parameters (duration, peak intensity), we do not find any unusual behaviour in the single and double ionization signals of helium.

Now, using equations (25), we have calculated the variation of the single-, sequential-double-, and direct-double-ionization yields as a function of laser detuning. The results are plotted in Figure 5. The laser intensity and the pulse duration have been taken to be 4.5×10^{11} W/cm^2 and 1 ps (Gaussian FWHM), respectively. Since the laser intensity is rather weak and the pulse duration rather long, ($\Gamma_{a_1}\tau_L \gg 1$), the profiles of the single- and sequential-double-ionization yields exhibit typical Fano shapes. On the other hand, the profile of the direct-double-ionization is practically Lorentzian, as equation (34) suggests. It is interesting to point out that, although ionization into the single continuum $|c_3\rangle$ and the double-continuum $|c_2\rangle$ do not interfere, as equation (33) shows, the contribution of the sequential-double-ionization represented by the first term of equation (33) can be made minimum if the laser frequency is tuned to the absorption minimum of the autoionizing state. Thus, the contrast ratio of the sequential- and direct-double-ionization is maximum when the laser is tuned to the absorption minimum.

4 Conclusion

We have calculated the single and double ionization of helium from the ground state around photon frequency 60.1 eV (in the vicinity of the AIS $|2s2p\rangle$) and for intensity of about 10^{16} W/cm^2. Both the photon frequency and the intensity are expected to be available with the Free Electron Laser (FEL) source at DESY in Hamburg. Our intention was to explore the role of the autoionization structure on the single and most importantly the double ionization yield. We have found that, for any pulse, the presence of the neighbouring autoionizing states $|2s2p\rangle$ and $|2s3p\rangle$ does not have any significant influence of the double ionization yield. It does, however, lead to an increase of the double to single ionization ratio in the case of a long pulse tuned to the absorption minimum of the $|2s2p\rangle$ state, because at that frequency, single-photon absorption is significantly reduced. This can be useful in reducing depletion of the initial state or perhaps even saturation of photoelectron detectors.

The work by T.N. was supported by the Grant-in-Aid for scientific research from the Ministry of Education and Science of Japan.

References

1. L.A.A. Nikolopoulos, P. Lambropoulos, J. Phys. B **34**, 545 (2001)
2. M.A. Kornberg, P. Lambropoulos, J. Phys. B **32**, L603 (1999)
3. J.S. Parker *et al.*, J. Phys. B **29**, L69 (2001)
4. D. Dundas, K.T. Taylor, J.S. Parker, E.S. Smyth, J. Phys. B **32**, L231 (1999)
5. J.S. Parker, L.R. Moore, D. Dundas, K.T. Taylor, J. Phys. B **33**, L691 (2000)
6. T. Nakajima, Phys. Rev. A **60**, 4805 (1999)
7. M. Goldberger, K. Watson, *Collision Theory* (Wiley, New York, 1964)
8. U. Fano, Phys. Rev. **124**, 1866 (1961)
9. P. Lambropoulos, P. Zoller, Phys. Rev. A **24**, 379 (1981)
10. P. Lambropoulos, P. Maragakis, J. Zhang, Phys. Rep. **305**, 203 (1998)